

# Controlling Acidity and Selectivity of HY-Type Zeolites by Silanation

E. Klemm, M. Seitz, H. Scheidat, and G. Emig

*Lehrstuhl für Technische Chemie I, Universität Erlangen-Nürnberg, Egerlandstrasse 3, D-91058 Erlangen, Germany*

Received June 5, 1997; revised September 8, 1997; accepted September 12, 1997

Silanation, which is the chemisorption of silane, allowed modification of the acidity and the pore size of HY zeolites. Nitrous oxide was used to stabilize the remaining SiH bonds after silanation by converting them into SiOH groups. In the case of 3-methylpentane cracking, the silanated oxidized samples exhibited a higher activity and a reduced deactivation rate at longer times on stream. Silanation of the HY zeolite without subsequent oxidation allowed almost total suppression of deactivation, especially in the disproportionation of ethylbenzene but also less markedly in the cracking of 3-methylpentane. This suppression of deactivation required avoiding hydrolysis of the SiH group under reaction conditions, and therefore the reactants needed to be absolutely free of traces of water. The maximum deposition of silica that could be reached in one silanation/oxidation step was about 10 wt% at 573 K. Higher temperatures were not possible because of the uncontrolled formation of polysilanes. Simultaneous silanation and oxidation, which means that the oxidant was already present during silanation, allowed controlled deposition degrees higher than 10 wt%. The high-silanated HY samples were found to exhibit shape selectivity in ethylbenzene disproportionation which was not observed on the parent samples. It was shown that pore blocking is the main reason for the decreasing activity with increasing silica deposition in the case of the high-silanated samples. The observed shape selective effects were comparable to those of ZSM-5-type zeolites. © 1998 Academic Press

## INTRODUCTION

To improve the performance of zeolites as molecular sieves or catalysts several modification techniques can be used. Ion exchange and dealumination are the most common methods used to change sorption properties and/or acidity of zeolites. In the last decade, the chemical vapor deposition (CVD) of silicon compounds has been a growing field of research and industrial interest (1).

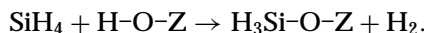
In 1973 McAteer and Rooney (2) reported that treatment with methylsilane in the gas phase allows modification of the acidity of HY zeolite. In 1977 Barrer *et al.* (3) investigated the silanation of faujasites and mordenites and characterized the modified samples by sorption measurements. Vansant (1) continued the investigations in this field but no catalytic measurements were presented. With the beginning of the 1980s many studies were performed concerning

so-called pore size engineering, i.e., the fine control of the pore opening size of zeolites. Niwa *et al.* (4) carried out CVD of silicon tetramethoxide on mordenite to reduce the size of the pore opening without affecting the acid properties. This was guaranteed by choosing a CVD precursor like silicon alkoxides that was larger than the pore opening. The mechanism was clarified several years later by the same authors (5). Silicon tetramethoxide reacts with the surface hydroxide and yields an anchored trimethoxide, which can react with a vicinal trimethoxide or with a tetramethoxide from the gas phase. Thus, a silica multilayer on the outer crystallite surface can be produced. In the 1990s the research in CVD modification focused on HZSM-5 zeolites and in the generation of *para*-selectivities for selective production of *para*-dialkylbenzenes [e.g., (6–8)]. Various Mobil patents [U.S. Patents 4,477,583 (1984) and 4,127,616 (1978)] show that it is of industrial interest to modify a molecular sieve catalyst with a silicon compound to achieve high *para*-selectivities in the conversion of toluene to xylene. Further improvement of that process was announced in a patent by Chang and Rodewald (9) who were cofeeding the silicon compound in the starting period of the production cycle. In the first hour the *para*-selectivity increased from 28 to 99% at 719 K, 500 psig, and 4.0 h<sup>-1</sup> WHSV. As the parent sample, a HZSM-5 zeolite with a modulus of 26 and a crystallite radius of 0.1 μm was used.

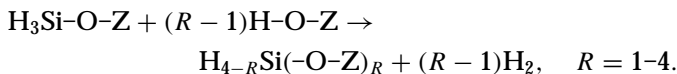
Very few studies have dealt with silane as a CVD precursor, though there are several advantages to using this precursor instead of silicon alkoxides. The chemisorption of silane yields a monolayer and, by subsequent oxidation and further silanation, multilayers can be produced. Silane is a compound that is small enough to penetrate the microporous system of large-pore (e.g., HY) and medium-pore (e.g., HZSM-5) zeolites. Thus, it is possible to control the location of deposition in principle by appropriate selection of operation conditions. Furthermore, compared with silicon alkoxides, no organic compounds are formed during chemisorption, and therefore, no coke must be burnt off.

Because of Barrer *et al.* (3) the following reaction steps can be distinguished during the modification with silane. In the first reaction step (primary reaction) silane reacts with one accessible zeolitic silanol group, such as terminal silanol

groups and bridged silanol groups:



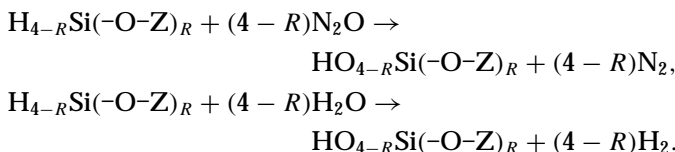
In secondary reactions the chemisorbed silane reacts with additional vicinal silanol groups:



$R$  denotes the molar ratio of hydrogen produced to silane consumed in the total silanation reaction. Thus, if the primary reaction occurs exclusively, the  $R$  value is one, whereas in the case of increasing secondary reactions, the  $R$  value increases up to a maximum value of 4.

Under ambient conditions the SiH bonds of the silanated zeolite sample are relatively stable compared with the SiH bonds of the free silane molecule. This can be seen from diffusive reflectance Fourier transform infrared spectroscopy (DRIFTS) measurements described later where the sample is silanated, purged, and subsequently contacted with air for several hours. Figure 1 shows that only a small fraction of the SiH bonds are oxidized at room temperature within 24 h.

For complete stabilization of the hydride functions, water vapor or nitrous oxide can be used for oxidation at elevated temperatures, thus transforming the hydride function into a terminal silanol group:



The aim of the present work was to prove that silane is an appropriate and advantageous CVD precursor for a controlled postsynthesis modification of HY zeolites. HY zeo-

lites often exhibit a strong loss of activity in hydrocarbon conversions due to coking, and as they are wide-pore zeolites, no shape selective effects occur in the conversion of small aromatics and paraffins. Thus, controlled silanation of HY zeolites was performed in the present study to reduce deactivation by coking and to generate a shape selective HY zeolite.

## EXPERIMENTAL

### Catalysts

The NaY (KM 580) zeolite was obtained from Degussa Company, Hanau, Germany. The total Si/Al ratio amounted to 2.8 and was determined both by a conventional chemical analysis and by X-ray photoelectron spectroscopy (XPS). By analyzing the  $^{29}\text{Si}$  MAS NMR spectrum of the parent sample (see Fig. 6) a framework Si/Al ratio of 4.8 was calculated. Thus, about 42% of the total aluminum exists as extraframework aluminum, which can also be deduced from the  $^{27}\text{Al}$  NMR spectrum shown later in Fig. 5. The size of the crystallites was about 1  $\mu\text{m}$ .

The H form was prepared by ion exchange with an ammonium chloride solution at 393 K and subsequent calcination at 823 K, which was repeated three times. By that procedure an exchange level of 85% was reached. Thus, the composition of the HY zeolite can be quantified with the following total formula:  $\text{H}_{28}\text{Na}_5[(\text{AlO}_2)_{33}(\text{SiO}_2)_{159}]$ . The powder was pelletized with 1% graphite as binding material, crushed, and sieved to 3-mm-size particles. Modification experiments and catalytic measurements using pellets produced without any binder showed no influence of the graphite binder on the modification process and catalytic behavior. Because of the low mechanical stability of such particles, high abrasion occurred which makes application of the binder material necessary.

For the purpose of comparison, a HZSM-5 zeolite was used in some catalytic measurements. This zeolite was obtained from Chemie Uetikon AG, Uetikon, Switzerland. The modulus was about 46, the sodium content lower than 0.1 wt%, and the radius 1  $\mu\text{m}$ . The corresponding total formula can be given as  $\text{H}_4[(\text{AlO}_2)_4(\text{SiO}_2)_{92}]$ .

### Silanation Procedure

Some safety precautions were necessary during silanation. Silane tends to combust spontaneously in contact with air. Thus, to avoid accidents the silane cylinder was placed outside the laboratory in an open-air area accessible only to specialist staff. The experimental setup itself was located in a special safety laboratory, with the control units being locally separated to control the experimental setup from a secure area.

Nitrogen as the carrier gas, silane as the CVD precursor, and nitrous oxide as the oxidant could be dosed

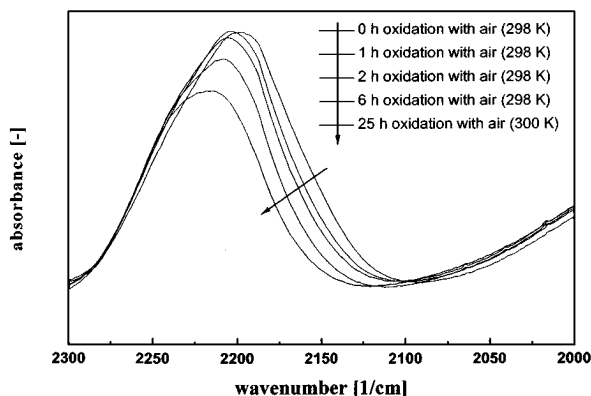


FIG. 1. Oxidation of the SiH bonds in a HY zeolite silanated at 465 K with air at room temperature proven by DRIFTS measurements (SiH IR band at 2200  $\text{cm}^{-1}$ ).

continuously through the reactor using thermal conductivity mass flow controllers. The reactor consisted of a heated tube of stainless steel into which a catalyst basket could be inserted. The zeolite pellets were inserted into the basket on a metal frit. Differential conversions guaranteed the absence of axial gradients inside the catalyst bed. A thermocouple inside the catalyst bed allowed isothermal conditions to be maintained. To adjust conditions below atmospheric pressure inside the reactor, a backpressure controller and a vacuum pump were installed. A hydrogen analyzer (LFE Analysentechnik) made it possible to measure the total amount of hydrogen formed during the chemisorption. In combination with the total amount of silica deposited the  $R$  value can be calculated.

About 4 to 5 g of the sample was introduced into the basket and heated to 623 K for more than 12 h *in vacuo*. Afterward, the sample was cooled to 423 K, the basket was transferred into an aluminum cartridge which was evacuated, and after further cooling to room temperature, the cartridge was weighed to obtain the dry mass of the zeolite. The basket was then transferred from the cartridge back to the reactor. Silanation was started after evacuation and heating up to the reaction temperature. To complete silanation the physically adsorbed silane and that remaining in the gas phase were removed by purging with nitrogen and by the use of vacuum. The subsequent oxidation was performed at 623 K for 1 h with nitrous oxide as oxidant. Under these conditions all hydride groups were oxidized as determined by DRIFTS measurements described later. Determination of the weight gain after silanation, on the one hand, and after oxidation, on the other hand, according to the cartridge procedure previously described allowed calculation of the percentage of silica deposited on the zeolite as well as calculation of the  $R$  value.

As an alternative to the subsequent oxidation procedure, oxidation and silanation were carried out simultaneously by feeding the reactor with a silane/nitrous oxide mixture.

### Catalytic Measurements

Ethylbenzene disproportionation was performed in a recycle reactor apparatus described elsewhere (10). The disproportionation of ethylbenzene was first introduced as a model reaction by Karge and Weitkamp to compare the activities of different zeolite catalysts and to distinguish between medium- and large-pore zeolites (11, 12). The reactor was filled with 2 g of the catalyst and operated at 523 K. The partial pressure of ethylbenzene in the feed was 330 mbar, with nitrogen being the carrier gas. The sample was dried at 523 K in a small nitrogen flux overnight prior to reaction.

Cracking of a 1:1 mixture of *n*-hexane and 3-methylpentane was carried out according to the instructions of Frilette *et al.* (13) in a stainless-steel flow reactor under isothermal conditions. Two grams of the catalyst was in-

troduced into the reactor. The reaction temperature was 573 K and the molar composition of the feed was 80% nitrogen, 10% *n*-hexane, and 10% 3-methylpentane. A gas chromatograph was used to analyze the reactor effluent.

### Solid-State MAS NMR

Solid-state MAS NMR spectra were obtained on a Bruker MSL-400 instrument (Institute of Chemical Technology I, University of Stuttgart, Stuttgart, Germany) operating at a  $^1\text{H}$  frequency of 400.1 MHz, a  $^{27}\text{Al}$  frequency of 104.3 MHz, and a  $^{29}\text{Si}$  frequency of 79.4 MHz. The spinning rates in all experiments were between 3.5 and 10 kHz. The signals were referenced to a 0.1 M aluminum nitrate solution in the case of  $^{27}\text{Al}$  spectra and to tetramethylsilane in the case of  $^1\text{H}$  and  $^{29}\text{Si}$  spectra.

The  $^1\text{H}$  resonance positions of hydroxyl protons in zeolites are in the chemical shift range 0–6 ppm (14). Terminal Si–OH groups appear at about 1.8 ppm, terminal AlOH groups at about 2.7 ppm, bridged OH groups in the supercage at about 3.9 ppm, and bridged OH groups in the sodalite cage at about 4.9 ppm. Several  $^{29}\text{Si}$  MAS lines occur depending on the number of aluminum atoms in the first coordination sphere of the silicon atom. Furthermore, it is possible to calculate the framework Si/Al ratio from the area of the individual lines. In the  $^{27}\text{Al}$  MAS NMR the line at 60 ppm is attributed to tetrahedral coordinated aluminum and the line at 0 ppm is attributed to octahedral coordinated extraframework aluminum.

### Temperature-Programmed Desorption of Ammonia

Temperature-programmed desorption (TPD) of ammonia was performed on an AMI-100 instrument (Altamira Instruments). The samples (50–70 mg) were first dried in a quartz U-tube in a helium stream at 773 K for 3 h and then exposed to 100 mbar of ammonia for 15 min at 373 K. Subsequently, the samples were purged at the same temperature with helium for 180 min. The ammonia TPD measurement was carried out from 323 to 1173 K at a heating rate of 10 K  $\text{min}^{-1}$ . Helium was used as carrier gas with a flow rate of 25  $\text{cm}^3 \text{min}^{-1}$ . The desorbed ammonia was detected with a thermal conductivity detector. A reference TPD spectrum of the sample without ammonia being adsorbed was subtracted. The pulse-calibration procedure with ammonia allowed quantification of the TPD signal.

### DRIFTS Measurements

The IR measurements were obtained by means of DRIFTS using a Perkin–Elmer Paragon 1000 FT-IR spectrometer equipped with a MCT detector, a “praying mantis” optical attachment, and a diffusive reflectance high-temperature cell from Harrick Scientific (Model HVC-DR2). The zeolite powder was introduced into the cup of the cell, which was operated via downward flow to

avoid possible fluidization of the catalyst. The spectral resolution was  $1\text{ cm}^{-1}$ .

### Micropore Volume Determination

The zeolite void volume was determined by means of physisorption of nitrogen at 77 K on an ASAP-2000 (Micromeritics) instrument. An improved Horvath-Kawazoe equation including spherical pore models (15) was used to calculate the cumulative micropore volume distribution. From the adsorbed gas volume corresponding to 20 Å, the micropore volume was derived by a conversion factor.

### Determination of the Coke Content

By means of thermogravimetry the coke content of the samples after catalytic measurements was determined. The soft coke was assigned to the weight loss between 473 and 813 K in nitrogen. The amount of hard coke was assigned to the weight loss after burning off the deposits at 813 K. The graphite binder was not oxidized under this condition.

## RESULTS AND DISCUSSION

### Low-Silanated Samples

The progress of silanation in time was determined by stopping silanation at various, but definite times and measuring the weight gain by the aforementioned procedure. At 465 K, approximately half of the final amount is deposited in the first 4 h, but to approach chemisorption equilibrium, at least 100 h are necessary (Fig. 2). For the silanation kinetics, a general multiple-site model was assumed and the following equation was derived:

$$\theta = 1 - \sum_i \varphi_i e^{-k_i t}$$

$\theta$  is the deposited amount normalized by its final value,  $\varphi_i$  is the fraction of acid sites of type  $i$ , and  $k_i$  is the rate constant of chemisorption at acid sites of type  $i$ . As can be seen

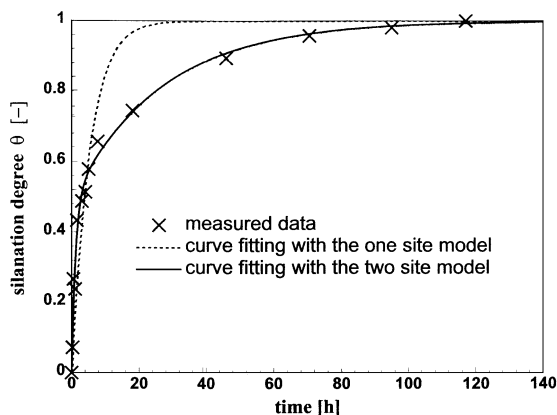


FIG. 2. Measured and predicted silanation kinetics at 465 K.

TABLE 1

Estimated Parameter Values of the Models Describing Silanation Kinetics

Physical quantity	Symbol	Unit	Value
One-site model			
Rate constant of chemisorption	$k$	$\text{h}^{-1}$	$0.19 \pm 30\%$
Two-site model			
Rate constant of chemisorption on strong acid sites	$k_s$	$\text{h}^{-1}$	$0.89 \pm 43\%$
Rate constant of chemisorption on weak acid sites	$k_w$	$\text{h}^{-1}$	$0.04 \pm 43\%$
Fraction of strong acid sites	$\varphi_s$	—	$0.49 \pm 19\%$

from Fig. 2 at least a two-site model is necessary to describe the silanation process (16). Table 1 summarizes the quantities of the model parameters obtained by regression. The fast initial stage of silanation must involve stronger acid sites, which are most likely the bridged OH groups in the supercages of the HY zeolite. It can be excluded that silanation of the easily accessible outer crystallite surface causes this fast initial silanation period because about 3.5 wt% is deposited in this period which is much more than one monolayer of silane on the outer crystallite surface.

The slower part of the silanation process is most probably induced by weakly acid terminal AlOH groups (extraframework aluminum) and terminal SiOH groups (outer surface, lattice defects). It is also possible that weakly acid bridged OH groups due to the heterogeneity of the acid sites (17) and that decreasing accessibility of the bridged OH groups due to the increasing amount of deposit contribute to the slow part of silanation.

In further preliminary investigations silanation was performed at different temperatures. After reaching chemisorption equilibrium the silanated sample was totally oxidized using nitrous oxide. Figure 3 shows that the amount of silica deposited increases with temperature,

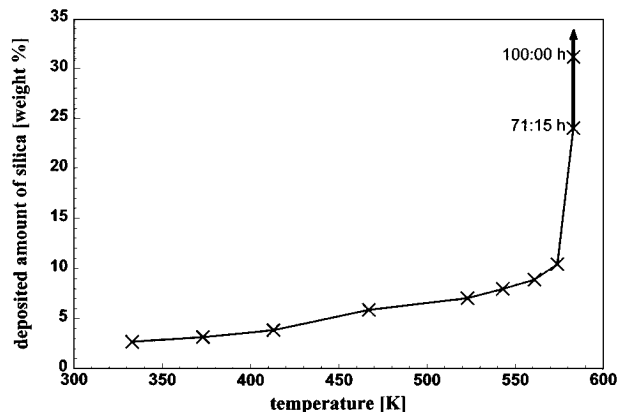


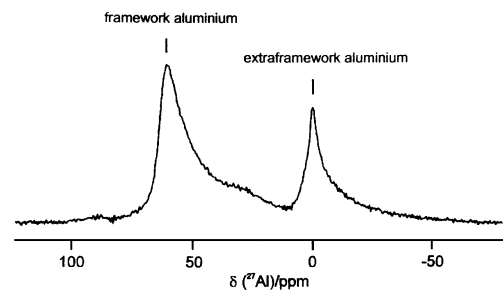
FIG. 3. Maximum possible amount of deposited silica depending on temperature.

which allows the conclusion that at higher temperatures, more sites are active enough to react with silane. Thus, it must be the weaker acid sites that cause the observed effect. Figure 3 also indicates that at temperatures higher than 573 K, multilayers are formed. At these temperatures silane can react with itself by forming polysilane compounds growing with time. Thus, no equilibrium value can be reached, which is elucidated in Fig. 3 with an arrow and with labels indicating the corresponding time of silanation. In all further investigations the parent samples were silanated at about 550 K. At this temperature the formation of polysilane could be avoided and the rate of deposition was maximum. After 3 h the silanation was stopped to avoid the slow part of the silanation process. A silica deposition of 5.1 wt% was reached.

*R* values of about 2.5 were calculated both from the weight gain and from the amount of hydrogen released during chemisorption. This indicates that secondary reactions occurred between one anchored silane molecule and a second or third OH group of the zeolite, which can be bridged OH groups or terminal AlOH groups of extraframework alumina which is present to a great extent.

To analyze the  $^1\text{H}$  NMR spectra (Fig. 4) it was assumed that the bridged OH groups in the sodalite cage remained

#### PARENT HY-SAMPLE:



#### SILANATED / OXIDIZED HY- SAMPLE:

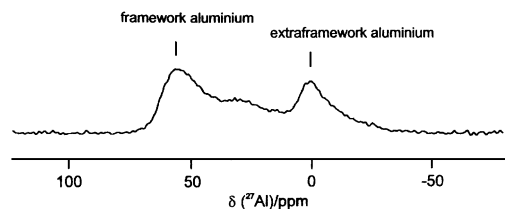
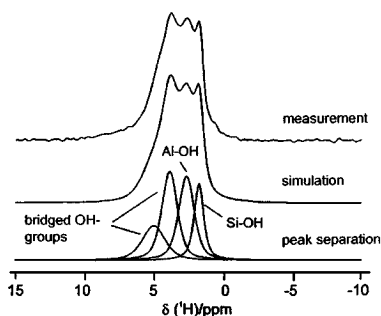


FIG. 5.  $^{27}\text{Al}$  MAS NMR spectra of the parent and silanated oxidized HY samples (5.1 wt% silica).

#### PARENT HY-SAMPLE:



#### SILANATED / OXIDIZED HY- SAMPLE:

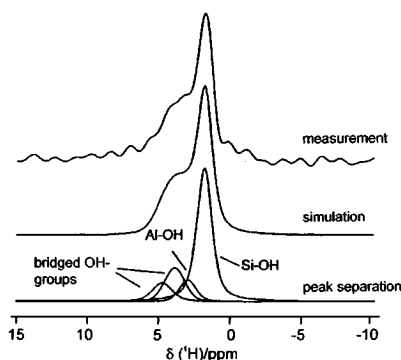


FIG. 4.  $^1\text{H}$  MAS NMR spectra of the parent and silanated oxidized HY samples (5.1 wt% silica).

unaffected during silanation because of their reduced accessibility. Working on this assumption the amount of bridged OH groups in the supercages is reduced only by 25%, the terminal AlOH groups are reduced by 50%, and the terminal SiOH groups increased by a factor of 3.5. This indicates that silane does not reach every bridged OH group in the supercages, probably because it is hindered by the extraframework aluminium. It can be further assumed that the secondary reactions occur between one silane molecule that has already reacted with a bridged OH group and the AlOH groups of the extraframework aluminium.

Comparing the  $^{27}\text{Al}$  MAS NMR (Fig. 5) spectra of the parent and the silanated/oxidized sample leads to the conclusion that the modification procedure does not cause significant further dealumination so that the increase in the SiOH line can be explained in this way. From the  $^{29}\text{Si}$  spectra (Fig. 6) it can be deduced that the anchored silicon forms a covalent SiOSi bond with the silicon of the zeolite framework because of the increasing SiOAl peak.

In Fig. 7 measured ammonia TPD spectra are depicted. The high-temperature peak at about 673 K can be assigned to strong Brønsted acid sites, whereas the low-temperature peak at about 480 K can be assigned to weakly adsorbed ammonia. It can be concluded that in the silanated nonoxidized sample, a stronger loss of Brønsted acidity occurs than after oxidation of the SiH bonds. After oxidation, Brønsted

## PARENT HY-SAMPLE:

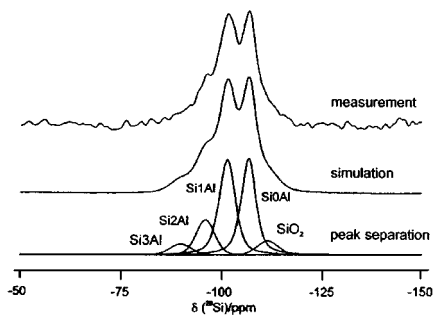
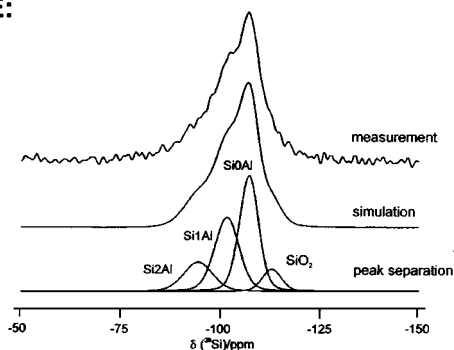
SILANATED / OXIDIZED  
HY- SAMPLE:

FIG. 6.  $^{29}\text{Si}$  MAS NMR spectra of the parent and the silanated oxidized HY samples (5.1 wt% silica).

acidity increases but does not reach the value of the unmodified sample. It is unlikely that the terminal silanol groups produced by oxidation are responsible for that increasing acidity. Thus, it is assumed that after silanation, the remaining bridged OH groups are only weakly acidic, because the partially negative charge of the hydrogen in the SiH group compensates via its electrical field the positive charge of the hydrogen in the neighboring bridged OH group. There-

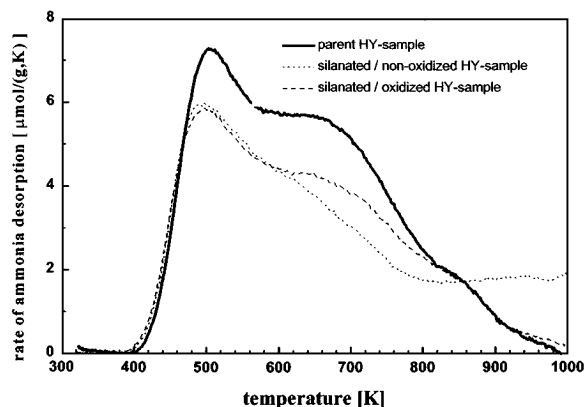


FIG. 7. Ammonia TPD spectra of the parent, silanated nonoxidized, and silanated oxidized HY samples (5.1 wt% silica).

fore, after oxidation the remaining OH groups get back their original acidity. Quantification of the loss of strong Brønsted acid sites due to the modification process by simulation of the spectrum and peak separation was not reliable. Therefore only relative effects have been discussed. Ammonia TPD shows that not all strong Brønsted acid sites have been destroyed by silanation/oxidation.

The observed TPD signal (thermal conductivity detector) of the silanated nonoxidized sample at temperatures above 800 K is caused by water. This was proven by injection of a gas sample taken from the outlet of the TPD apparatus into the mass spectrometer.

The catalytic performance of the samples was tested in the disproportionation of ethylbenzene and in the cracking of 3-methylpentane and *n*-hexane. Because of the low silanation level (about 10 wt%) shape selective effects did not occur. Thus, the investigations on the low-silanated samples focused on their deactivation behavior. The modified samples exhibited a lower activity in the initial stage of all reactions compared with the parent sample (Figs. 8–10). The order of the initial activities of the samples corresponds to the order of the amounts of Brønsted acid sites measured by ammonia TPD (see Fig. 7); i.e., the silanated/oxidized sample is more active than the silanated/nonoxidized sample and both are less active than the unmodified sample.

From the viewpoint of industrial applications, long-time behavior often is more important. Comparing Figs. 8, 9, and 10 leads to the conclusion that the silanated oxidized samples exhibit a slightly smaller deactivation rate only in the case of 3-methylpentane cracking. In the case of ethylbenzene disproportionation and cracking of *n*-hexane, the same decrease in conversion with time was observed at long times on stream. In the latter two cases, coke formation and the main reaction seem to occur on the same strong acid sites

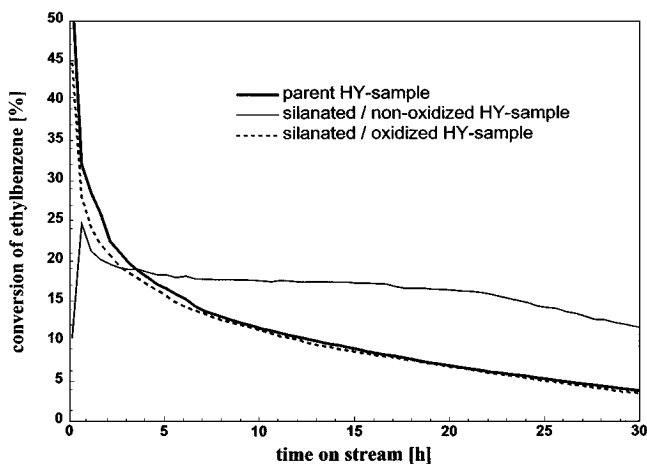


FIG. 8. Ethylbenzene disproportionation on the parent, silanated nonoxidized, and silanated oxidized HY samples (5.1 wt% silica). Reaction temperature: 523 K, partial pressure of ethylbenzene: 330 mbar, modified residence time: 50 g · h/mol.

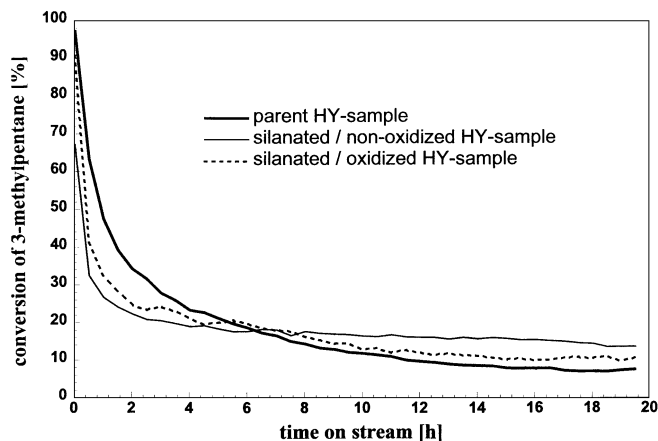


FIG. 9. Cracking of 3-methylpentane on the parent, silanated nonoxidized, and silanated oxidized HY samples (5.1 wt% silica). Reaction temperature: 573 K; partial pressure: 100 mbar *n*-hexane, 100 mbar 3-methylpentane; modified residence time: 87 g · h/mol.

so that selective inhibition of the coke formation reaction is not possible. Thus, deposition of silica prior to reaction and deposition of coke during reaction have the same impact on activity. This can also be concluded from Fig. 11, where the amounts of hard and soft coke of the different samples are illustrated. The amount of soft coke is approximately the same in all samples; only the amount of hard coke is reduced due to the space occupied by the deposited silica.

In the cracking of 3-methylpentane weaker acid sites are involved so that removal of the unselective strong acid sites by silanation is successful.

The silanated nonoxidized sample exhibits the best long-term performance in the ethylbenzene disproportionation (see Fig. 8) and in the cracking of 3-methylpentane (see

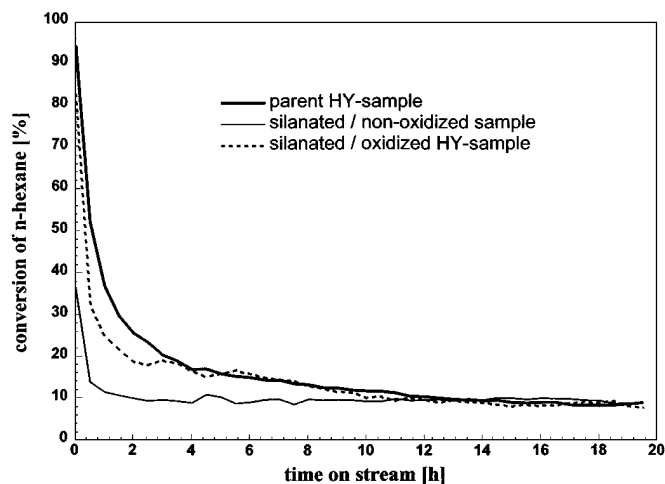


FIG. 10. Cracking of *n*-hexane on the parent, silanated nonoxidized and silanated oxidized HY samples (5.2 wt% silica). Reaction temperature: 573 K; partial pressure: 100 mbar *n*-hexane, 100 mbar 3-methylpentane; modified residence time: 87 g · h/mol.

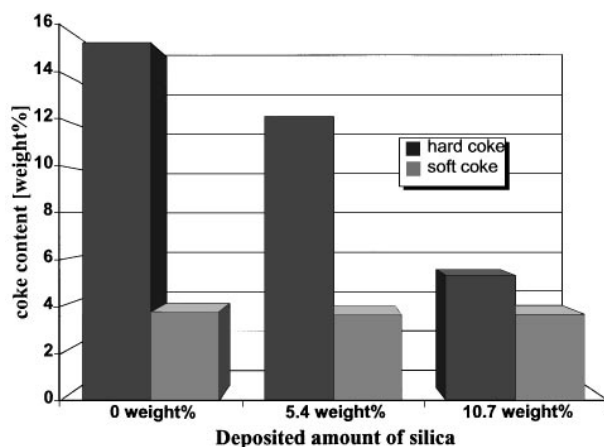


FIG. 11. Amount of hard coke and soft coke on different modified samples compared with the parent sample after 16 h onstream in ethylbenzene disproportionation at 523 K.

Fig. 9). The activity remains at a high and almost constant value for a long time on stream, especially in the case of ethylbenzene disproportionation. By making DRIFTS measurements and monitoring the SiH band it can be concluded that the final observed decrease in activity after 20 h time on stream (see Fig. 8) was induced by hydrolysis of the SiH group by traces of water in the ethylbenzene. Thus, if it is possible to avoid hydrolysis by drying the reactants to a high degree, activity will remain at a high and constant value also after 20 h. The partially negative charge of the hydrogen in the SiH groups may enhance the desorption of unsaturated compounds which act as coke precursors. An equilibrium between desorption and production of the coke precursors is reached and deactivation cannot progress.

### High-Silanated Samples

According to Weitkamp *et al.* (18) no *para*-selectivity could be observed in the disproportionation of ethylbenzene at the parent HY zeolite. Also, in the low-silanated samples no *para*-selective effects occurred. Thus, silica depositions higher than 10 wt% have to be achieved to check if *para*-selective effects can be generated in these high-silanated samples. To reach this goal, silanation and oxidation were performed simultaneously which means that a mixture of nitrous oxide and silane was fed into the reactor. During silanation, the SiH groups of the anchored silane are converted into silanol groups, which in turn react further with silane. From Fig. 12 it is evident that high-silanated samples can be produced in a relatively short period. Already after 4 h of modification a deposition degree of 10 wt% was exceeded. In the long-term region a lower but constant deposition rate indicates the complete consumption of the strong acid sites of the zeolite and the formation of multilayers. This is in accordance

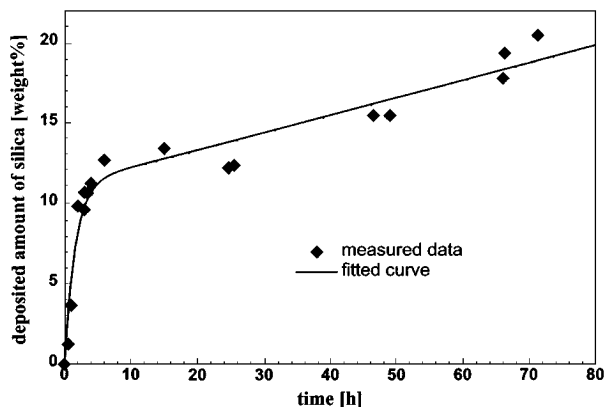


FIG. 12. Measured weight gain versus duration of the simultaneous silanation and oxidation at 573 K.

with the already discussed results of separate silanation and oxidation (see Fig. 3), where a maximum amount of 10 wt% was reached at 573 K, which is the same temperature as in the simultaneous silanation and oxidation presented in Fig. 12. The micropore volume during simultaneous silanation and oxidation was determined by measuring nitrogen sorption isotherms at 77 K and analyzing them by a modified Horvath–Kawazoe method (16). Figure 13 clearly indicates that a linear correlation exists between the degree of deposition and the corresponding micropore volume. This confirms the assumption that the deposition occurs predominantly inside the microporous system. Ammonia TPD measurements of high-silanated samples are illustrated in Fig. 14. At silica depositions larger than approximately 8.7 wt% the total amount of acid sites remains constant because silanation occurs on the terminal SiOH groups of the silica already deposited, and thus the number of acid sites does not change anymore.

Ethylbenzene disproportionation was performed in the recycle reactor apparatus by running a temperature ramp (dynamic method) at 15 K/h. In Fig. 15 the measured con-

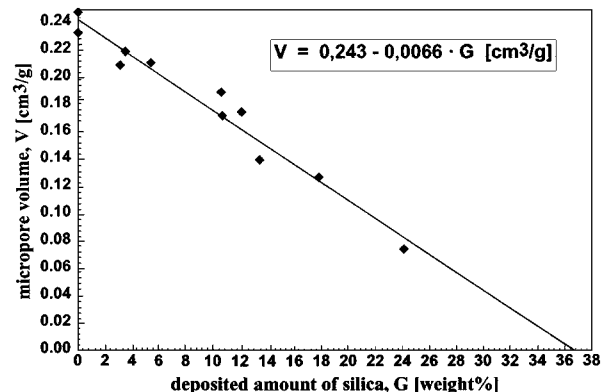


FIG. 13. Correlation between the degree of silica deposition and the corresponding micropore void volume.

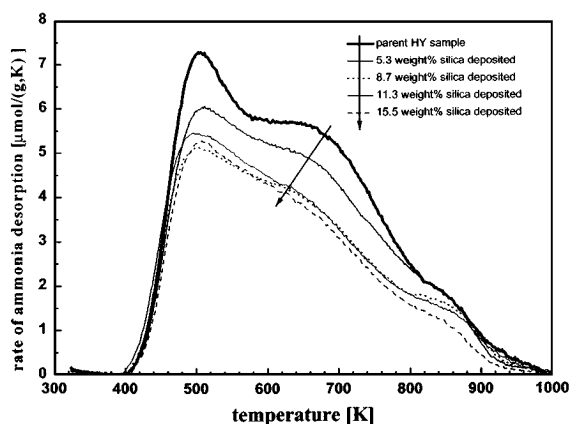


FIG. 14. Ammonia TPD of high-silanated samples.

versions and in Fig. 16 the corresponding *para*-selectivities are plotted versus temperature. For the purpose of comparison, results on a HZSM-5 zeolite are also included. Using the unmodified HY sample, conversion apparently decreases with increasing temperature because strong coke formation, which is progressing with time, dominates the increase in the reaction rate due to the temperature rise. Using the HZSM-5 sample, deactivation is a minor influence and the exponential temperature dependence of the rate constant causes the usual increase in conversion with increasing temperature. The HY sample modified with 15.5 wt% silica also exhibits increasing conversion with increasing temperature as long as the temperature does not exceed 533 K. Above 533 K, coking suddenly begins to dominate, and with further increasing temperature, the conversion decreases slightly. Nevertheless, it remains at higher values compared with the unmodified sample. The sample containing 17.8 wt% silica showed, over the entire temperature region, increasing conversion (see Fig. 15). The

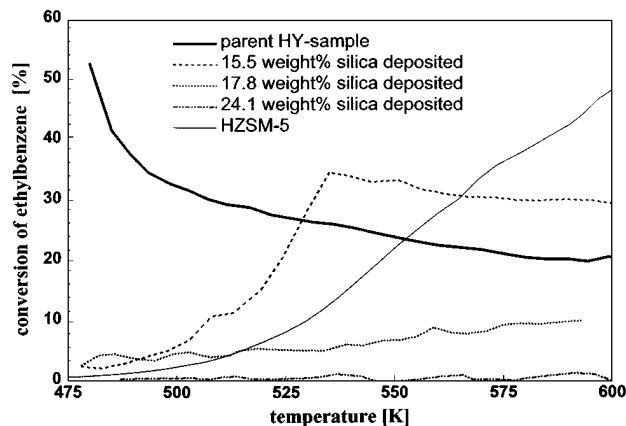


FIG. 15. Conversion versus time in ethylbenzene disproportionation on HY samples containing various amounts of silica and on HZSM-5. Temperature ramp: 15 K/h, partial pressure of ethylbenzene: 330 mbar, modified residence time: 50 g · h/mol.



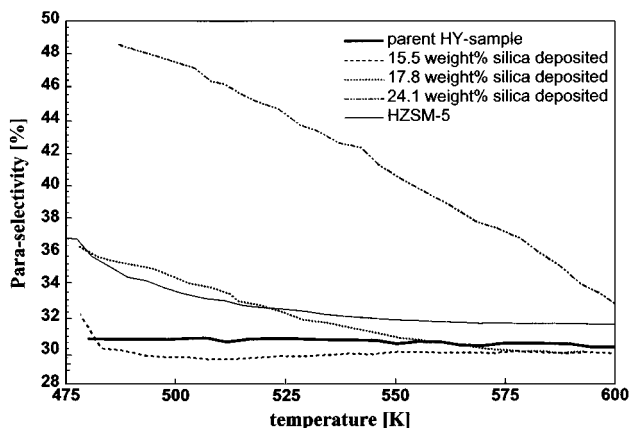


FIG. 16. *para*-Selectivity versus time in ethylbenzene disproportionation on HY samples containing various amounts of silica and on HZSM-5. Partial pressure of ethylbenzene: 330 mbar, modified residence time: 50 g · h/mol.

conversion on HZSM-5 lies at most temperatures between the 15.5 wt% sample and the 17.8 wt% sample. This is accord with the remaining void volume of these samples being almost equivalent to the void volume determined for the HZSM-5 sample, which was about  $0.12 \text{ cm}^3 \text{ g}^{-1}$ . When 24.1 wt% was deposited on the parent sample the conversion was nearly zero.

Considering the results of ammonia TPD (Fig. 14) allows the conclusion that in the high-silanated samples, pore blocking is the main reason for the decrease in activity with increasing deposition of silica because the amount of acid sites remains constant. Also, the suddenly starting deactivation at 533 K for the sample containing 15.5 wt% silica can be explained by geometric constraints. At temperatures higher than 533 K, the activation energy for the formation of coke precursor can be overcome. This activation energy must be very high because of the geometric constraints and thus deactivation starts abruptly.

As can be seen in Fig. 16, the sample containing 17.8 wt% silica showed almost the same *para*-selectivity versus temperature dependence as the HZSM-5 sample. A distortion by different conversion levels can be neglected because up to 513 K, the modified sample showed slightly higher conversions but also slightly higher *para*-selectivities. It is well known that *para*-selectivity should increase with decreasing conversion (19). The high *para*-selectivities of the sample containing 24.1 wt% silica can be explained by the very low conversion level close to zero. Thus, these high *para*-selectivities are caused not only by the geometric constraints of the deposit but also by the primary selectivity combined with low subsequent isomerization activity.

## CONCLUSIONS

The investigations presented demonstrate clearly that silanation/oxidation is an appropriate technique to reach

a controlled improvement of the catalytic performance of HY zeolites. Analysis of  $^1\text{H}$  MAS NMR spectra and ammonia TPD spectra of the parent and the silanated oxidized samples allowed the conclusion that only about 25% of the bridged OH groups in the supercages of the parent sample were involved in silane chemisorption. This was explained by the reduced accessibility due to the large amount of 40% extraframework aluminum. By  $^1\text{H}$ ,  $^{27}\text{Al}$ , and  $^{29}\text{Si}$  solid-state MAS NMR, the mechanism of silanation was elucidated. Silane was anchored at an acidic OH group and secondary reactions followed because an *R* value of about 2.5 was determined. Most probably the SiH groups remaining after the first reaction step reacted with ALOH groups of the extralattice aluminum which were reduced to about 50% by silanation. New covalent SiOSi groups were formed as can be seen from the  $^{29}\text{Si}$  MAS NMR. By subsequent oxidation the remaining SiH bonds were converted into terminal silanol groups. Applying ammonia TPD it was found that the silanated nonoxidized samples possess lower acidities than the silanated oxidized samples. Because of the low acidity of the terminal silanol groups this can be explained only by the hydride property of the SiH bond destroying, via its electrical field, the acidity of the remaining bridged OH groups.

An obvious improvement in deactivation behavior was obtained with the silanated nonoxidized samples. Activity remained at a high and constant level, especially in ethylbenzene disproportionation but also in 3-methylpentane cracking. The enhanced long-term stability could be ascribed to the existence of Si-H bonds because the hydride enhances the desorption of coke precursors. Thus, hydrolysis of these bonds must be avoided, which means that the reactants must be free of any trace of water.

High-silanated samples were achieved by simultaneous silanation and oxidation with deposition degrees higher than 10 wt%. By ammonia TPD measurements it could be deduced that pore blocking is the reason for the reduced activity and not the decrease in acid sites which remained constant.

Deposit of at least 16 wt% silica on the HY zeolite was necessary to obtain *para*-selectivities larger than thermodynamic equilibrium. The possibility that the enhanced *para*-selectivity was caused by conversion effects was ruled out. The *para*-selectivities were comparable to those measured on a HZSM-5 zeolite. In the 24.1 wt% sample, conversion was almost zero and the large *para*-selectivities observed were also induced by the primary selectivity which dominates at extremely low conversion levels.

## ACKNOWLEDGMENTS

The authors gratefully acknowledge the financial support provided by the Deutsche Forschungsgemeinschaft. We are particularly obligated to Dr. Engelhardt and Dr. Feuerstein (Institute of Chemical Technology I,

University of Stuttgart, Stuttgart, Germany) for conducting the solid state MAS NMR measurements.

## REFERENCES

1. Vansant, E. F., "Pore Size Engineering in Zeolites." Wiley, New York, 1990.
2. McAteer, J. C., and Rooney, J. J., in "Molecular Sieves," pp. 258–265. Am. Chem. Soc., Washington, DC, 1973.
3. Barrer, R. M., Jenkins, R. G., and Peeters, G., in "Molecular Sieves—II," pp. 258–270. Am. Chem. Soc., Washington, DC, 1977.
4. Niwa, M., Kato, S., Hattori, T., and Murakami, Y., *J. Chem. Soc. Faraday Trans. 1* **80**, 3135 (1984).
5. Niwa, M., Kawashima, Y., Hibino, T., and Murakami, Y., *J. Chem. Soc. Faraday Trans. 1* **84**, 4327 (1988).
6. Kim, J.-H., Ishida, A., Okajima, M., and Niwa, M., *J. Catal.* **161**, 387 (1996).
7. Bhat, Y. S., Das, J., Rao, K. V., and Halgeri, A. B., *J. Catal.* **159**, 368 (1996).
8. Cejka, J., Zilkova, N., Wicherlova, B., Eder-Mirth, G., and Lercher, J. A., *Zeolites* **17**, 265 (1996).
9. Chang, C. D., and Rodewald, P. G., U.S. Patent 5,498,814 (1996).
10. Klemm, E., Scheidat, H., and Emig, G., *Chem. Eng. Sci.* **52**, 2757 (1997).
11. Karge, H. G., Ladebeck, J., Sarbak, Z., and Hatada, K., *Zeolites* **2**, 94 (1982).
12. Karge, H. G., Ernst, S., Weihe, M., Weiss, U., and Weitkamp, J., *Stud. Surf. Sci. Catal. C* **84**, 1805 (1994).
13. Frilette, V. J., Haag, W. O., and Lago, R. M., *J. Catal.* **67**, 218 (1981).
14. Engelhardt, G., *Stud. Surf. Sci. Catal.* **58**, 285 (1991).
15. Cheng, L. S., and Yang, R. T., *Chem. Eng. Sci.* **49**, 2599 (1994).
16. Scheidat, H., Ph.D. dissertation, University of Erlangen-Nuremberg, 1997.
17. Datka, J., Broclawik, E., and Klinowski, J., *Stud. Surf. Sci. Catal. C* **84**, 2187 (1994).
18. Weitkamp, J., Ernst, S., Jacobs, P., and Karge, H. G., *Erdoel Kohle Erdgas Petrochem.* **39**, 13 (1986).
19. Vinek, H., and Lercher, J., *J. Mol. Catal.* **64**, 23 (1991).